Reconstruction of the reconnection rate from Cluster measurements: First results

V. S. Semenov,[1] T. Penz,[2,3] V. V. Ivanova,[1] V. A. Sergeev,[1] H. K. Biernat,[2,3] R. Nakamura,[2] M. F. Heyn,[4] I. V. Kubyshkin,[1] and I. B. Ivanov[5]

Received 11 April 2005; revised 23 June 2005; accepted 8 August 2005; published 22 November 2005.

[1] A model of transient time-dependent magnetic reconnection is used to describe the behavior of nightside flux transfers (NFTEs) in the Earth's magnetotail. On the basis of the analytical approach to reconnection developed by Heyn and Semenov (1996) and Semenov et al. (2004a) we calculate the magnetic field and plasma bulk velocity time series observed by a satellite. The solution for the plasma parameters is given in the form of a convolution integral. The calculation of the reconnection electric field is an ill-posed inverse problem, which we treat in the frame of the theory of regularization. This method is applied to Cluster measurements from 8 September 2002, where a series of earthward propagating 1-min scale magnetic field and plasma flow variations are observed outside of the plasma sheet, which are consistent with the theoretical picture of NFTEs. We analyzed three NFTEs and reconstructed the reconnection electric field. Additionally, the position of the satellite with respect to the reconnection site as well as the Alfvén velocity are estimated because they are necessary input parameters for the model. The reconnection electric field is found to be about 1–2 mV/m, while the reconnection site is located about 29–31 R_E in the magnetotail.

Citation: Semenov, V. S., T. Penz, V. V. Ivanova, V. A. Sergeev, H. K. Biernat, R. Nakamura, M. F. Heyn, I. V. Kubyshkin, and I. B. Ivanov (2005), Reconstruction of the reconnection rate from Cluster measurements: First results, *J. Geophys. Res.*, *110*, A11217, doi:10.1029/2005JA011181.

1. Introduction

[2] In a search for reconnection at the dayside magnetopause using magnetic field data from ISEE 1 and 2 spacecrafts, *Russell and Elphic* [1978] noticed that there appear localized transient reconnection events, which can be identified by an isolated bipolar variation of the magnetic field component normal to the magnetopause and a simultaneous deflection in the tangential components, which can be interpreted as disturbances caused by a moving flux tube passing by the satellite (Figure 1a). They named these characteristic events "flux transfer events" (FTEs). Also, *Haerendel et al.* [1978] reported in situ measurements of transient reconnection at high-latitude dayside magnetopause from HEOS 2 satellite.

[3] After the observation of these FTE signatures, some attempts were made to reconstruct different features of the reconnection process involved in the generation of FTEs. *Southwood* [1985] predicted that FTE signatures would be observed by a satellite regardless of whether or not it actually penetrates the FTE. *Farrugia et al.* [1987] verified Southwood's suggestion and reproduced the magnetic field signatures outside the flux tube by considering the flow of an inviscid, incompressible plasma over a semicircular cylinder. They showed that FTE-like signatures could be generated without the satellite is penetrating the obstacle. *Walthour et al.* [1993, 1994] used a deHoffmann-Teller (HT) frame, which is only valid if the structure of the FTE does not alter significantly over the timescale of the encounter with a satellite (several minutes). Using this property, they developed a method based on integral transforms for inferring the cross-sectional size, shape, and the speed of propagation of a thin, infinitely long obstacle corresponding to a flux tube (Figure 1b). Since the analysis is confined to perturbations outside the obstacle, the method is referred to as a remote sensing method.

[4] Another approach to this topic was used by several authors [*Hau and Sonnerup*, 1999; *Hu and Sonnerup*, 2001, 2003] who developed a method based on the Grad-Shafranov equation to reconstruct two-dimensional space plasma structures in magnetohydrostatic equilibrium (Figure 1c). *Hu and Sonnerup* [2003] applied this model to two magnetopause crossings by the spacecraft AMPTE/IRM and reconstructed magnetic field structures. *Sonnerup et al.* [2004] used this method to give a rough estimation of the reconnection rate. However, the propagation of a reconnected flux tube can rather be described by the inertia force of the plasma and the Maxwellian tension, which is

[1]Institute of Physics, State University St. Petersburg, St. Petersburg, Russia.
[2]Space Research Institute, Austrian Academy of Sciences, Graz, Austria.
[3]Also at Institute of Physics, University of Graz, Graz, Austria.
[4]Institute for Theoretical Physics, Technical University Graz, Graz, Austria.
[5]Petersburg Nuclear Physics Institute, Gatchina, Russia.

0148-0227/05/2005JA011181$09.00

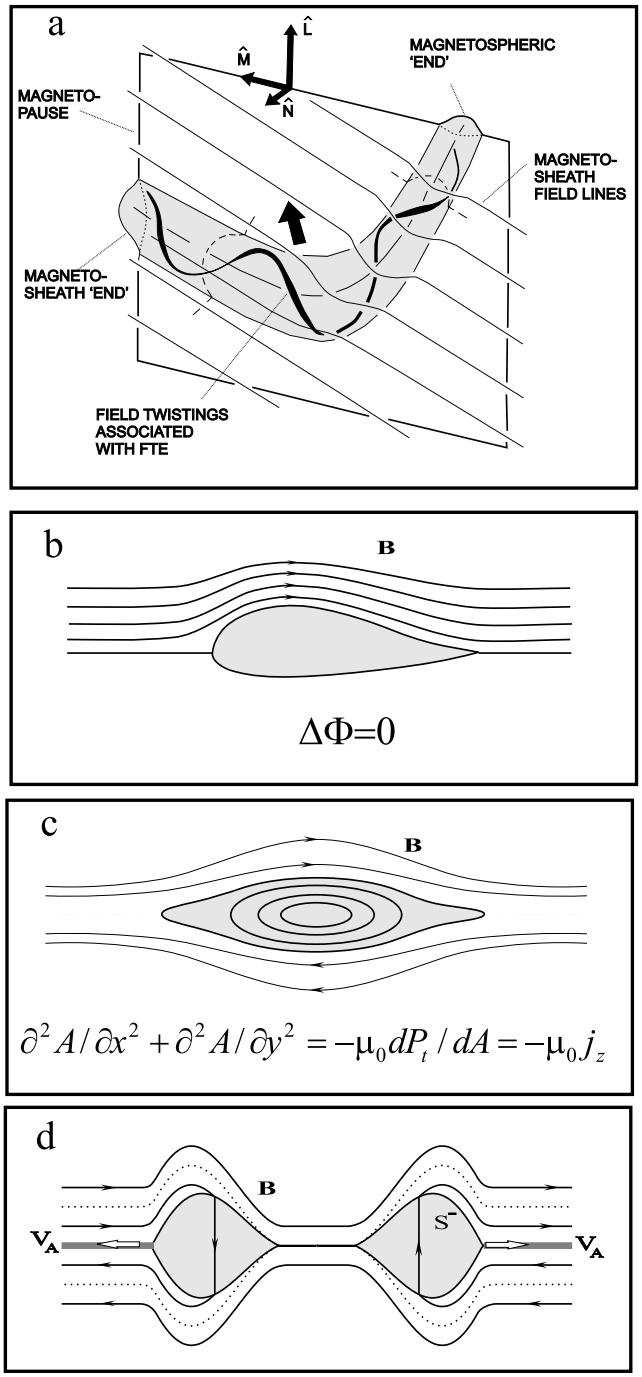

Figure 1. Different approaches to describe and analyze flux transfer events (FTEs). (a) The original sketch by *Russell and Elphic* [1978], (b) the potential flow method used by *Walthour et al.* [1993, 1994], (c) the approach using the Grad-Shafranov equation to calculated structures in magnetohydrostatic equilibrium [*Sonnerup et al.*, 2004], and (d) the model of transient Petschek-type reconnection [*Biernat et al.*, 1987; *Semenov et al.*, 1992]. It can be seen that only the last approach is directly associated with the reconnection of magnetic field lines and therefore allows to reconstruct the reconnection rate.

essentially a time-dependent process, and therefore this process can be hardly understood in a magnetohydrostatic approach.

[5] In order to describe the temporal evolution of FTEs, time-dependent Petschek-type models of reconnection were developed [e.g., *Biernat et al.*, 1987; *Semenov et al.*, 1992, 2004a, 2004b; *Heyn and Semenov*, 1996]. Figure 1d shows the switch-off stage in the time-dependent model of magnetic reconnection. Here, reconnection is initiated by the appearance of an electric field in a localized region of the current sheet separating oppositely directed magnetic fields. Owing to this process, reconnection-associated disturbances are propagating along the current sheet in the form of pairs of shocks moving in opposite direction away from the reconnection site. These shocks bound a region of heated and accelerated plasma, the so-called outflow region (the shaded areas in Figure 1d). After the electric field has dropped to zero, the shocks detach from the reconnection site and continue to propagate along the current sheet, which can be seen in Figure 1d. It should be noted that even the reconnection process ceased, energy conversion still takes place, leading to a continued growth of the outflow region.

[6] *Lawrence et al.* [2000] analyzed a series of FTE-like events generated by a time-dependent model of reconnection, where they studied the effects of different reconnection pulses on the perturbations. Recently, *Semenov et al.* [2005] developed a theoretical model to reconstruct the reconnection rate out of perturbations of the ambient magnetic field for an incompressible plasma. It is shown that an inverse method based on the representation of the disturbances in form of convolution integrals works satisfactory for reasonable distances and magnetic field parameters.

[7] FTE-like structures appear also in the Earth magnetotail, which was investigated by *Sergeev et al.* [1987] in order to explain phenomena related with magnetospheric substorms. They performed a qualitative comparison between measurements of ISEE 1 within the plasma sheet and model predictions from a transient reconnection model, which showed a general agreement. In later work, these events were referred to as nightside flux transfer events (NFTEs) [*Sergeev et al.*, 1992]. These are short-term events in the substorm-time plasma sheet, which can be described by impulsive variations of the reconnection rate in models of transient reconnection. Such structures noticed in the tail plasma sheet are often referred to as individual bursts of BBF, as transient plasma sheet expansions, as plasmoids or flux ropes, as well as NFTEs [*Sergeev et al.*, 1992; *Ieda et al.*, 1998; *Slavin et al.*, 2003]. The appearance of reconnection structures in the magnetotail was also confirmed by several other satellite observations, like Geotail [*Nagai et al.*, 2001] or Cluster [*Runov et al.*, 2003].

[8] We apply our model to a series of earthward propagating NFTEs observed by the Cluster satellites on 8 September 2002 shortly after 2120 UT. At this time, the four satellites were located in the magnetotail at [−16.7; 0.2; 4.5] R_E GSM clearly outside of the plasma sheet. In a recent paper, *Sergeev et al.* [2005] argued that the observed features can be interpreted as NFTEs. Therefore we select these events for the data analysis done in this paper.

[9] The purpose of this paper is a further development of the flux tube model in order to reconstruct the reconnection

electric field. It is organized as follows. In the following section, we describe the direct problem based on the Cagniard-deHoop method [*Lamb*, 1904; *Cagniard*, 1939; *deHoop*, 1960; *Heyn and Semenov*, 1996; *Semenov et al.*, 2004a], which allows to calculate the disturbances in the ambient plasma environment. Using this method, the magnetic field and velocity components are found to be convolution integrals of the reconnection rate and an integration kernel, which includes the magnetic field parameters and the distance information. We show that the plasma and magnetic field perturbations are in agreement with the picture proposed for NFTEs.

[10] In section 3, the theoretical background used for the reconstruction of the reconnection rate out of these parameters is shown. The ill-posed inverse problem is treated in the frame of Tikhonov regularization [*Tikhonov and Arsenin*, 1977]. A quantitative discussion of the influence of the distance between the observation point and the reconnection site is given.

[11] Section 4 deals with the application of the method to measurements of the Cluster satellites (compare with *Sergeev et al.* [2005]). Features indicating that NFTEs are appearing in Cluster measurements on 8 September 2002 are discussed. Using the method described here, we are able to reconstruct the reconnection electric field from Cluster measurements on 8 September 2002 out of magnetic field measurements. Additionally, we present a rough estimation of the distance between the satellite and reconnection site. Also, possible improvements of the method by expanding the theoretical model for a compressible plasma are discussed.

2. Direct Problem for Incompressible Plasma

[12] For our purpose, we consider the structure of the Earth's magnetotail as oppositely directed magnetic fields, which are separated by an infinitely thin tangential discontinuity, the plasma sheet. Across a tangential discontinuity, the normal components of the magnetic field and plasma velocity are zero ($B_n = 0$, $v_n = 0$). To fulfill the Rankine-Hugoniot relations, the density and the tangential components of the magnetic field and velocity may change arbitrarily, subject only to the requirement that the total pressure, which is the sum of the thermal and the magnetic pressure, $p + B^2/(8\pi)$, stays constant [*Heyn et al.*, 1988]. Since there is no mass flow and no magnetic connection across a tangential discontinuity, there will be no electric field component along it ($E_t = 0$). If we assume that the plasma conductivity decreases in a certain region, the generation of a reconnection electric field, and therefore a normal component of the magnetic field will follow [*Biernat et al.*, 1987]. Any local deviation of the perfect conductivity approximation due to the reconnection electric field will cause a reconfiguration of the tangential discontinuity. The surface gets nonlinearly unstable and decays into a system of MHD wave modes.

[13] To simplify the problem, we introduce the restriction of so-called weak reconnection [*Petschek*, 1964] which implies that the reconnection electric field $E(t)$ is much smaller than the Alfvén electric field $E_A = v_A B_0/c$, where B_0 and $v_A = B_0/\sqrt{4\pi\rho}$ are the initial magnetic field and the Alfvén velocity, respectively. Within this restriction, we are considering small components of the magnetic field and velocity in a direction normal to the tangential discontinuity:

$$B_n^2 \ll B_t^2, \tag{1}$$

$$\rho v_n^2 \ll p + \frac{B_t^2}{8\pi}. \tag{2}$$

Thus to lowest order, the total pressure is conserved across the discontinuity. As a result, there is no pressure gradient that could drive a strong fast shock. Further, in the incompressible case ($\rho = const$), which is considered in the following, the Alfvén wave merges with the slow shock, forming a so-called Petschek shock (S^-, Figure 1d). These Petschek shocks bound a region of accelerated and heated plasma, the field reversal or outflow region. After some time, the reconnection electric field has dropped to zero and the outflow regions become detached from the diffusion region and continue to propagate along the tangential discontinuity. These propagating shocks are causing disturbances in the ambient plasma environment, which can be measured by a satellite. In the following, we will show how these measured disturbances can be calculated by using a time-dependent Petschek-type model of transient magnetic reconnection.

[14] To study the problem of symmetric reconnection in an incompressible plasma (ρ = const) away from the reconnection line, the ideal magnetohydrodynamic (MHD) equations in normalized form [*Semenov et al.*, 2005]

$$\frac{\partial \mathbf{v}}{\partial t} + (\mathbf{v}\cdot\nabla)\mathbf{v} = -\nabla P + (\mathbf{B}\cdot\nabla)\mathbf{B}, \tag{3}$$

$$\frac{\partial \mathbf{B}}{\partial t} = \nabla \times (\mathbf{v}\times\mathbf{B}), \tag{4}$$

$$\nabla\cdot\mathbf{v} = 0, \tag{5}$$

$$\nabla\cdot\mathbf{B} = 0, \tag{6}$$

can be used. Here, $\mathbf{B}$ denotes the magnetic field, and $\mathbf{v}$ is the bulk velocity of the plasma. The background magnetic field $\mathbf{B^{(0)}}$ and the total pressure P are assumed to be constant. Additionally, we consider a fixed plasma, meaning that $\mathbf{v^{(0)}} = 0$ in the inflow region in zero order. The normalization is done with respect to the initial magnetic field $B^{(0)}$, the initial Alfvén velocity v_A, the time duration of a reconnection pulse $T^{(0)}$, the Alfvén electric field $E_A = v_A B^{(0)}/c$, and the length scale $v_A T^{(0)}$.

[15] A solution for this problem can be found by introducing a displacement vector as

$$\mathbf{v} = \frac{\partial}{\partial t}\boldsymbol{\xi}, \tag{7}$$

and

$$\mathbf{B} = \left(\mathbf{B^{(0)}}\cdot\nabla\right)\boldsymbol{\xi}. \tag{8}$$

After a Fourier-Laplace transformation of the MHD equations and the introduction of the displacement vector, its z component fulfills an ordinary differential equation, giving a solution for the displacement vector in Fourier-

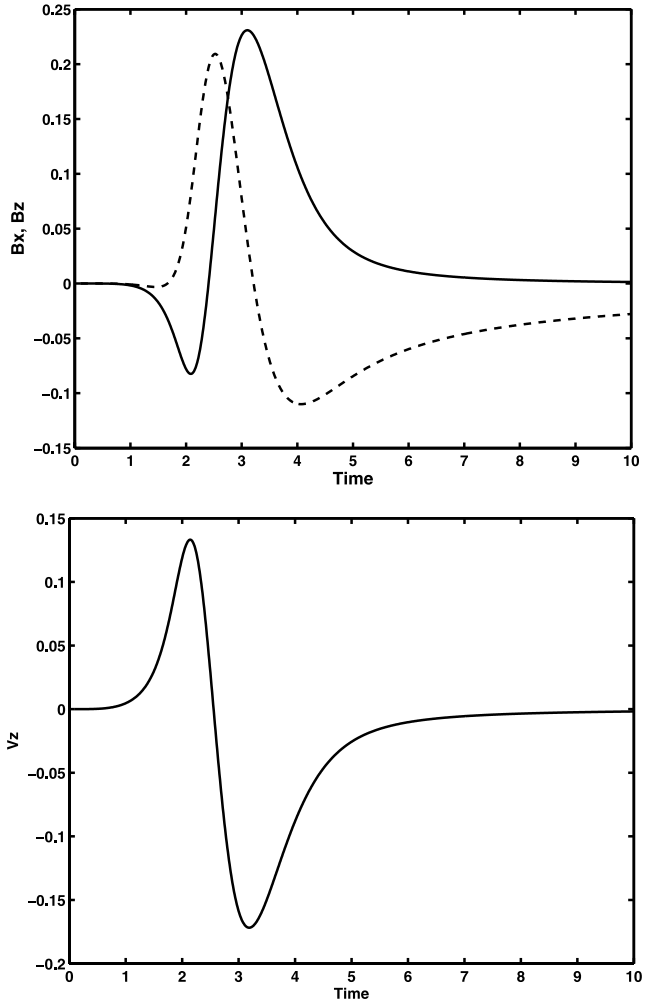

Figure 2. Shown are (top) the x component (dashed line) and the z component (solid line) of the magnetic field perturbations and (bottom) the z component of the plasma velocity.

Laplace space (see Appendix A). To get the displacement vector in time-coordinate space, we use the Cagniard-deHoop method [*Heyn and Semenov*, 1996]. It allows to perform the inverse Fourier transformation analytically, while the inverse Laplace transformation can be rewritten in form of a convolution integral (Appendix A). From this representation of the displacement vector, the magnetic field and plasma flow perturbations can be derived from equations (7) and (8).

[16] The z component of the magnetic field perturbations is found as

$$B_z(x,z,t) = -\frac{4}{\pi}\Re\int_0^t \frac{i\tau^3}{\left(q^2+\tau^2\right)^2}E(t-\tau)\,d\tau\,. \tag{9}$$

The x component of the magnetic field perturbations is found be combining equations (8) and (6), giving

$$B_x(x,z,t) = -B^{(0)}\frac{\partial}{\partial z}\xi_z = -\frac{4}{\pi}\Re\int_0^t \frac{\tau^3}{\left(q^2+\tau^2\right)^2}E(t-\tau)\,d\tau\,. \tag{10}$$

The z component of the plasma velocity follows directly from equation (7) as

$$v_z(x,z,t) = \frac{\partial}{\partial t}\xi_z = -\frac{4}{\pi B^{(0)}}\Re\int_0^t \frac{\tau^2 q}{\left(q^2+\tau^2\right)^2}E(t-\tau)\,d\tau\,, \tag{11}$$

while the x component is

$$v_x(x,z,t) = \frac{\partial}{\partial t}\xi_x = \frac{4}{\pi B^{(0)}}\Re\int_0^t \frac{i\tau^2 q}{\left(q^2+\tau^2\right)^2}E(t-\tau)\,d\tau\,. \tag{12}$$

Figure 2 shows time series of both magnetic field components (upper panel) as well as the z component of the velocity (lower panel) evaluated by using equations (9)–(11). The used electric field is of the form

$$E(t) = \frac{b^2 e^2}{20}\,t^2\,e^{-bt}\,, \tag{13}$$

with $b = 4$. The characteristic asymmetric bipolar variation expected for the B_z component is clearly visible, and also the deflection of the x component of the magnetic field. Additionally, the velocity behaves as proposed for NFTEs, with a upward flow of plasma in the beginning, followed by a strong flow directed the downward to the plasma sheet. Moreover, the maximum of the B_x component is correlated with a change in sign of the other components, which is a characteristic feature for NFTEs [*Sergeev et al.*, 1992, 2005].

[17] The bipolar variation of the normal component B_z can be explained by considering a bulge passing by the satellite (for a magnetopause context see *Russell and Elphic* [1978]). First, one can observe a change of the normal component reaching a maximum at the steepest slope of the bulge followed by a return to zero when the bulge reaches its maximum displacement. After that the bulge is propagating away from the satellite position, leading to a perturbation in the opposite direction and a return to zero afterward. Since the bulge is associated with reconnection in our model, the downward motion is also caused by reconnection, leading to a slightly asymmetric bipolar variation (Figure 2). The motion of the plasma can be interpreted in the following way: the leading edge of the shock front is causing a shift of the plasma away from the current sheet, giving the upward plasma flow. After the bulge passed by, a convective flow directed to the plasma sheet can be observed. In Figure 3, the z component of the magnetic field perturbations for different z distances of the observer is shown. For large normalized distances of $z > 1$ (to achieve the dimensional distance, the values must be multiplied by $v_A T^{(0)}$), the features are becoming small, which limits the method to distances smaller than about $z = 2$.

3. Inverse Problem

[18] An inverse problem can be seen as a model of a phenomenon characterized by ζ, which belongs to a certain space of models Z. Furthermore, let u be the observed

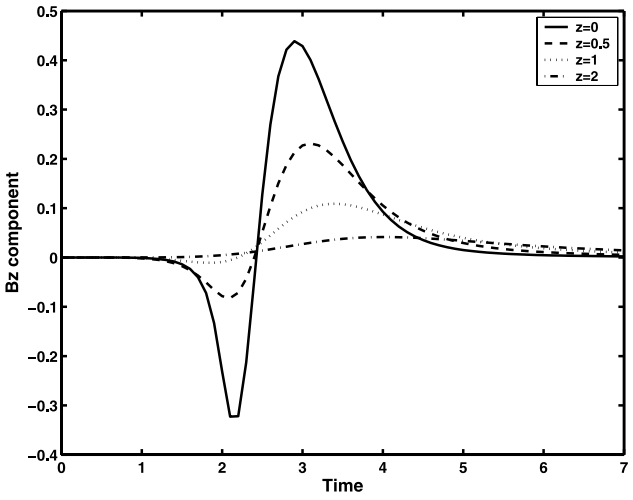

Figure 3. Time series of the z component of the magnetic field perturbations calculated at $z = 0$ (solid line), $z = 0.5$ (dashed line), $z = 1$ (dotted line), and $z = 2$ (dashed-dotted line).

indirect attributes of the phenomenon with $u \in U$. An operator A relates the two values by

$$A\zeta = u.$$

As a rule, the ζ attributes cannot be directly observed.

[19] The main job when solving an inverse problem is to find out whether the chosen model is compatible with the experimental data. The mathematical difficulty of solving such problems is that the inverse operator A^{-1} defined throughout its domain $AZ \subset U$ is not continuous. Hence there is the conventional division into the classes of well-posed and ill-posed problems. A well-posed problem, as defined by *Hadamard* [1932], must meet the requirements that (1) equation $A\zeta = u$ is solvable for the entire space U, (2) the solution is unique, and (3) the solution is stable, meaning that small perturbations of u result in small perturbations of the solution. For ill-posed problems, requirements 1 and 3 are not fulfilled. These kinds of problems can be solved by using the theory of regularization, which we apply in the following.

[20] To reconstruct the reconnection electric field from the magnetic field, we apply a Laplace transformation to the convolution integral (9) giving [*Semenov et al.*, 2005]

$$B_z(p) = K(p)E(p), \tag{14}$$

where $K(p)$ represents the kernel of the convolution integral. Thus the reconnection electric field is given as $E(p) = B_z(p)/K(p)$. For large p both $B_z(p)$ and $K(p)$ tend to zero, leading to oscillations in the result. To avoid this problem, we introduce a regularization parameter $M(p)$ [*Tikhonov and Arsenin*, 1977] so that

$$E(p) = \frac{B_z(p)}{K(p) + M(p)}. \tag{15}$$

The regularization operator $M(p)$ is defined as

$$M(p) = \begin{cases} 0 & |p| < R_{\max} \\ \infty & |p| > R_{\max} \end{cases}. \tag{16}$$

This operator does not influence the electric field for small values of p, but when the functions tend to zero for large p ($p > R_{\max}$), the denominator goes to infinity so that the reconnection electric field is zero in Laplace space and large oscillations are suppressed. The value of $R_{\max}$ is found from internal parameters of the numerical Laplace transformation. In Figure 4, the reconstructed electric field for different distances of the observer above the reconnection line is shown. The reconstructed electric fields correspond to the B_z components achieved from the direct problem and shown in Figure 3. One can see that for z distances below 0.5 the initial electric field and the reconstructed one nearly coincide. Up to 1 normalized length scale, the reconstruction method works well and gives quantitatively good results. For larger distances, qualitatively good results can be achieved; nevertheless the amplitude of the reconnection electric field cannot be reconstructed properly.

4. Example of Application: Substorm on 8 September 2002

[21] On 8 September 2002, an isolated substorm with a peak AE of about 400 nT occurred between 2000 and 2300 UT. A favorable constellation of multiple spacecraft and ground observations allowed to reconstruct in details the time sequence of this substorm and to model the near-Earth magnetic configuration, see *Sergeev et al.* [2005]. Following this description, a clear growth phase was observed after the arrival of a southward IMF after 2000 UT. The auroral breakup, the intensification of a westward electrojet, and Pi2 pulsations consistently indicated the expansion phase onset at 2118 UT in the 2200–2400 MLT sector. The Cluster tetrahedron was centered in the middle of the magnetotail at [−16.7; 0.2; 4.5] R_E GSM. The satellites exited from the thinning plasma sheet shortly after 2100 UT; they were located outside of the plasma sheet at the time of interest. After 2117 UT, a series of earthward propagating 1 min scale variations of the magnetic field and plasma flow components consistent with the picture of multiple NFTEs/flux ropes were observed (Figure 5). The first NFTE appeared at about 2117 UT and propagated earthward at a speed V_x = 625 km/s; V_y = −72 km/s (determined from timing of magnetic variations) [*Sergeev et al.*, 2005]. After this NFTE, the plasma sheet continued to be thin for some 20 min until the transient plasma sheet expansions start to be observed. This is a favorable situation because if the plasma sheet is thin, the approximation of a tangential discontinuity as an initial state is better justified. We applied our model to the NFTEs starting at 2121 UT, 2122:30 UT, and 2124 UT, ignoring the first NFTE at 2117 UT (in which the interaction of reconnected flux tube with previously closed plasma sheet flux tubes should be more pronounced than in the following development).

[22] A comparison with the results of the theoretical model (Figure 2) shows that the expected features for the perturbations are indeed found in the observations: the

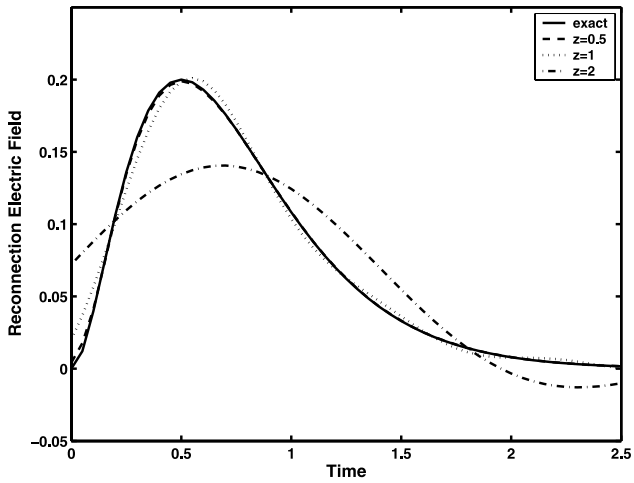

Figure 4. The reconstructed electric field for distances z = 0.5 (dashed line), z = 1 (dotted line), and z = 2 (dashed-dotted line) of the observer. The solid line indicates the initial electric field.

asymmetric bipolar variation of B_z, a compression of B_x, as well as a plasma flow v_z of cold O^+ ions directed to the plasma sheet are clearly visible. Also the change of the sign of B_z and v_z corresponds to the maximum in B_x. Therefore we suppose that the observed perturbations can be treated in the frame of our theoretical model.

[23] The GSM magnetic field data are obtained from the fluxgate magnetometer (FGM) experiment [*Balogh et al.*, 2001] with 1 s time resolution. The O^+ moments with 4 s time resolution were measured by the Composition and Distribution Function Analyzer (CODIF) of the Cluster Ion Spectrometry (CIS) experiment [*Rème et al.*, 2001] observed at the Cluster spacecrafts. The O^+ data was only used if the O^+ density exceeded 0.005 cm^{-3}. To evaluate the integration kernel $K(p)$, we also need to know the spacecraft location with respect to the reconnection site (Figure 6). Fortunately, the actual z position of the neutral sheet (about +1 R_E in z direction) is known from the modeling made by *Sergeev et al.* [2005]. Therefore the z distance between the satellite and the reconnection site is approximately 3.5 R_E.

[24] The determination of the x distance is done by using a global minimization routine. In our time-dependent model this is possible because according to (A5), the shape of the shock is changing if the x distance from the reconnection site is increasing. We use the measured B_z component as an input data, calculate the electric field in Laplace space, which should be strictly positive, but since we do not know the x distance it can appear negative somewhere. Therefore we take the module of the electric field and recalculate $\tilde{B}_z$ out of it. This procedure can be summarized as

$$B_z(t) \Rightarrow B_z(p) \Rightarrow E(p) \Rightarrow E(t) \Rightarrow |E(t)| \Rightarrow \tilde{B}_z(t).$$

Then we minimize the difference between $B_z(t)$ and $\tilde{B}_z(t)$ with a least squares approach in order to find the x distance as the value of x where the difference between the initial and the reconstructed magnetic field is a minimum. We limit the search to distances less than 35 R_E, which corresponds to the region of the near Earth neutral line (NENL), where reconnection most likely takes place. The local velocity of the disturbances is determined by using multipoint timing analysis [e.g., *Harvey*, 1998], giving about 700 km/s. We assume that this velocity is approximately the Alfvén velocity. Additionally, this analysis shows that the propagation velocity is directed mainly earthward in x direction with a small y component, which is a preferable configuration for our two-dimensional model.

[25] Since we know the Alfvén velocity, it is possible to introduce dimensional quantities. The background magnetic field is $B^{(0)}$ = 50 nT, the characteristic timescale is $T^{(0)}$ = 60 s, and the characteristic velocity is v_A = 700 km/s. This gives a characteristic length scale of $L = v_a T^{(0)}$ = 42,000 km ≈6.6 R_E. This means that one normalized length unit used in the theoretical description in section 2 corresponds to 6.6 R_E for this special case.

[26] Application of our model to the NFTE starting at 2121 UT in Figure 7 leads to a reconnection electric field of 2.1 mV/m over a time period of about 30 s (Figure 7) from C1. The location in x direction was found to be 12.5 R_E tailward of the satellite, corresponding to a location of the reconnection site at 29.2 R_E in the magnetotail. From C2 a reconnection rate of 1.5 mV/m and a distance to the reconnection site is 13.2 R_E, giving a distance to Earth of 29.9 R_E. C3 gives a reconnection rate of 1.6 mV/m at

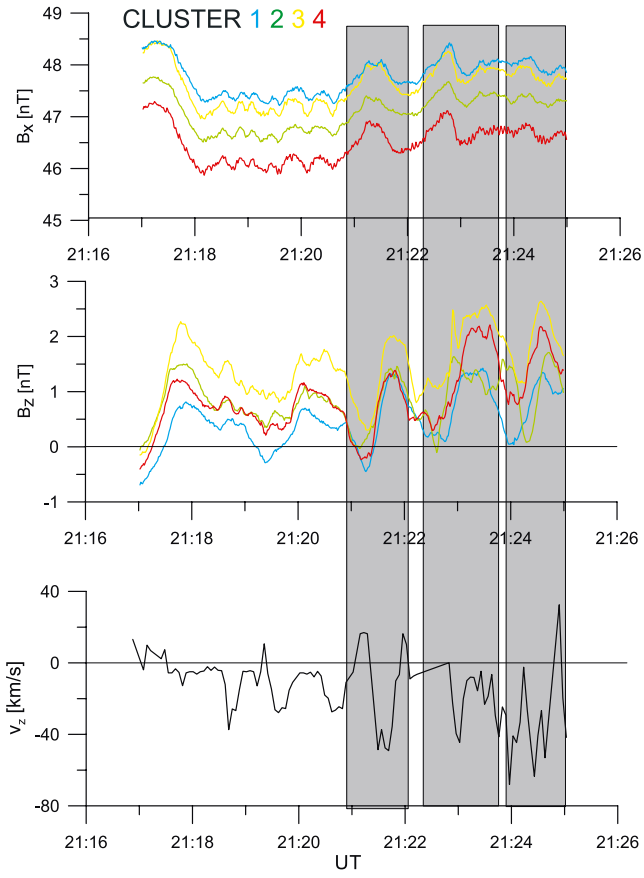

Figure 5. The event on 8 September 2002 observed by the four Cluster satellites. We analyze the nightside flux transfer events (NFTEs) starting at 2121 UT, at 2122:30 UT, and at 2124 UT (shaded areas).

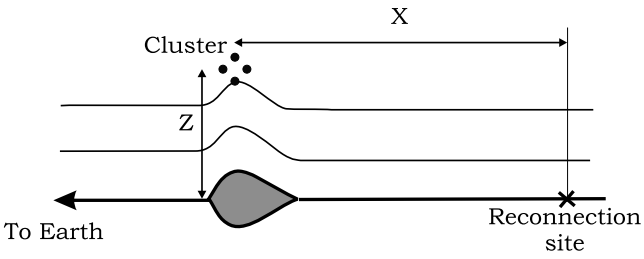

Figure 6. Scheme of the satellite location compared with the reconnection site. The z distance is estimated and the x distance is reconstructed.

a distance of 14 R_E. This implies a reconnection site at 30.7 R_E in the magnetotail. Finally, from C4 a reconnection rate of 1.6 mV/m at a x distance of 14.2 R_E from the satellite, corresponding to a reconnection site 30.9 R_E tailward of the Earth. Recapitulating, the reconnection rate is found to be between 1.5 and 2.1 mV/m, while the location of the reconnection site is between 29.2 and 30.9 R_E in the magnetotail.

[27] One can see that the reconstructed amplitude of the reconnection electric field and the reconnection site are consistent among the four satellites. For example, C3 is located about 0.5 R_E lower than C2; therefore the observed amplitude in the magnetic field perturbation at C3 is 1.7 nT compared with 1.3 nT at C2. Yet, the reconstructed amplitude of the electric field is quite similar, that is, 1.6 mV/m from C3 and 1.5 mV/m from C2. Therefore our model shows that the observed features at all four satellites are associated with the same reconnection event.

[28] The reconstructed electric field for the NFTE at 2122:30 UT from C1 is 0.9 mV/m with a time duration of about 20 s (Figure 8). Again the location of the reconnection site is at 29.2 R_E in the magnetotail. C2 gives a reconnection rate of 1.4 mV/m and at a distance of 13.3 R_E, giving the location of the reconnection site at 30 R_E. We do not use C3 for the reconstruction because the NFTE signal is not well pronounced. From C4, a reconnection rate of 1 mV/m at 12.8 R_E is found. The reconnection site is therefore located at 29.5 R_E in the magnetotail. Summarizing these results, the reconnection rate is between 0.9 and 1.4 mV/m and located between 29.2 and 30 R_E.

[29] The reconstructed electric field for the NFTE starting at 2124 UT from C1 is 1.2 mV/m with a time duration of about 30 s (Figure 9). The reconnection process took place about 11.9 R_E tailward from the satellite, giving the reconnection site at 28.6 R_E. From C2, the reconnection rate is found to be 1.4 mV/m, starting 12.6 R_E tailward. Therefore the reconnection site is located at 29.3 R_E. The reconnection rate obtained from C3 is 1.2 mV/m at the same location as found from C2. Finally, C4 gives the reconnection rate as 1.6 mV/m and a distance between the reconnection site and the satellite of 13 R_E. Thus the reconnection site is at 29.7 R_E. From this event, the reconstructed reconnection rate is between 1.2 and 1.6 mV/m, and the reconnection site is at 28.6 to 29.7 R_E in the magnetotail.

[30] The amplitude of the reconnection electric field is consistent with estimations of the magnetotail reconnection rate using ground-based measurements [*Blanchard et al.*, 1996, 1997; *Østgaard et al.*, 2005]. The smaller pulses which can be seen in Figures 7 and 8 for times larger than 30 s are noise, resulting from the solution of the inverse problem. The amplitude of the noise mainly depends on the z distance between the satellite and the reconnection structure [*Semenov et al.*, 2005]. If the z distance decreases, also the amplitude of the noise is decreasing.

5. Discussion and Conclusion

[31] In this work we present a first attempt to reconstruct the reconnection electric field from satellite measurements in an incompressible plasma. In order to apply the theoretical model to measured data, it is necessary to know crucial quantities like the distance between the satellite and the reconnection site or the Alfvén velocity. However, the

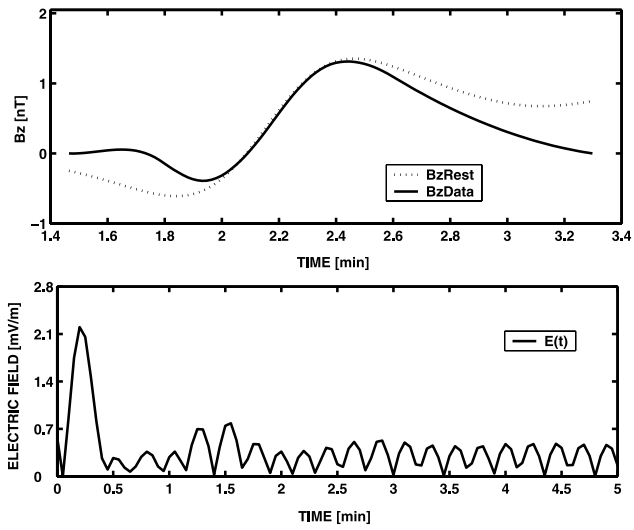

Figure 7. The reconnection electric field for NFTE starting at 2121 UT (lower panel), and initial (solid line) and reconstructed magnetic field perturbations (dashed line) using C1.

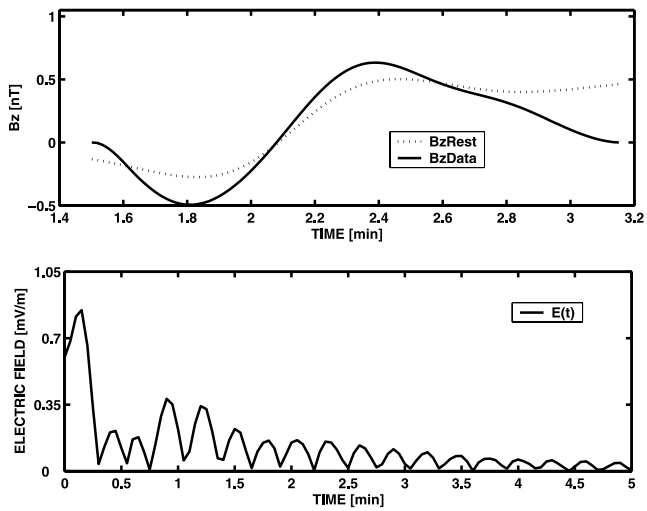

Figure 8. The reconnection electric field for NFTE starting at 2122:30 UT (lower panel), and initial (solid line) and reconstructed magnetic field perturbations (dashed line) using C1.

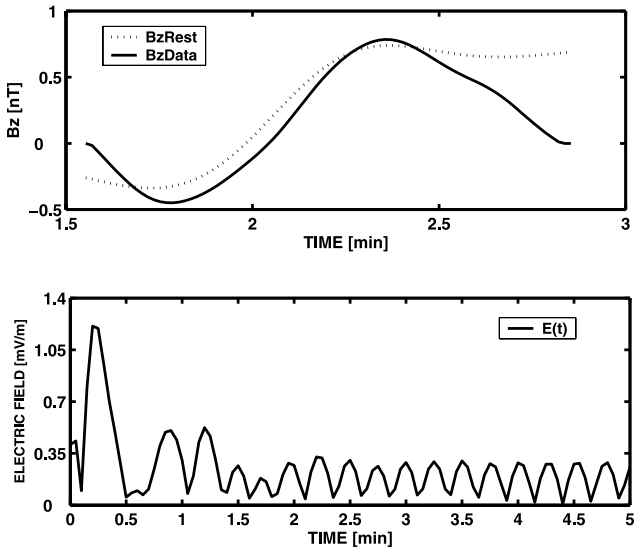

Figure 9. The reconnection electric field for NFTE starting at 2124 UT (lower panel), and initial (solid line) and reconstructed magnetic field perturbations(dashed line) using C1.

application of an analytical model requires to make some simplifications, which should be mentioned in the following.

[32] The x distance between the satellite and the reconnection site is determined by using a minimization routine. There exists the possibility that more that one minimum occurs, meaning that there is no single solution for the problem considered. In this case, the routine may give a wrong result. To avoid this problem, we applied our method only to the range of x distances where reconnection most likely takes place, namely the NENL to a distance less than 35 R_E, and run it with different starting points. It should be noted that a small difference in the x distance does not influence the shape of the disturbances significantly.

[33] We assume that the perturbations in the magnetic field are moving approximately with Alfvén velocity. Additionally, we assume that there is a homogeneous background density in the magnetotail. If the density changes significantly between the point of observation and the starting point of the disturbances, the estimated Alfvén velocity may differ from the real one. Since the Alfvén velocity is used for the normalization of the length scales, a variation of the Alfvén velocity will also give a variation of the spatial distances. If the Alfvén velocity decreases, also the length scales will decrease. From this discussion one can see that we know the values of these parameters only with some uncertainties, which should be minimized by further studies on this topic.

[34] Another simplification is the assumption of the incompressibility of the plasma. To visualize the effects of plasma compressibility, we applied a compressible direct model for a given electric field [*Heyn and Semenov*, 1996; *Semenov et al.*, 2004a] and calculated the magnetic field and plasma velocity and compared it with the results of the incompressible model (Figure 10). From this comparison it is possible to derive some tendencies. One can see that the magnitude of the B_z component remains approximately the same. This is because of the fact that the variations of the B_z component mainly depend on the inclination of the shock, which bounds the outflow region. Since the inclination is very similar for both the compressible and incompressible

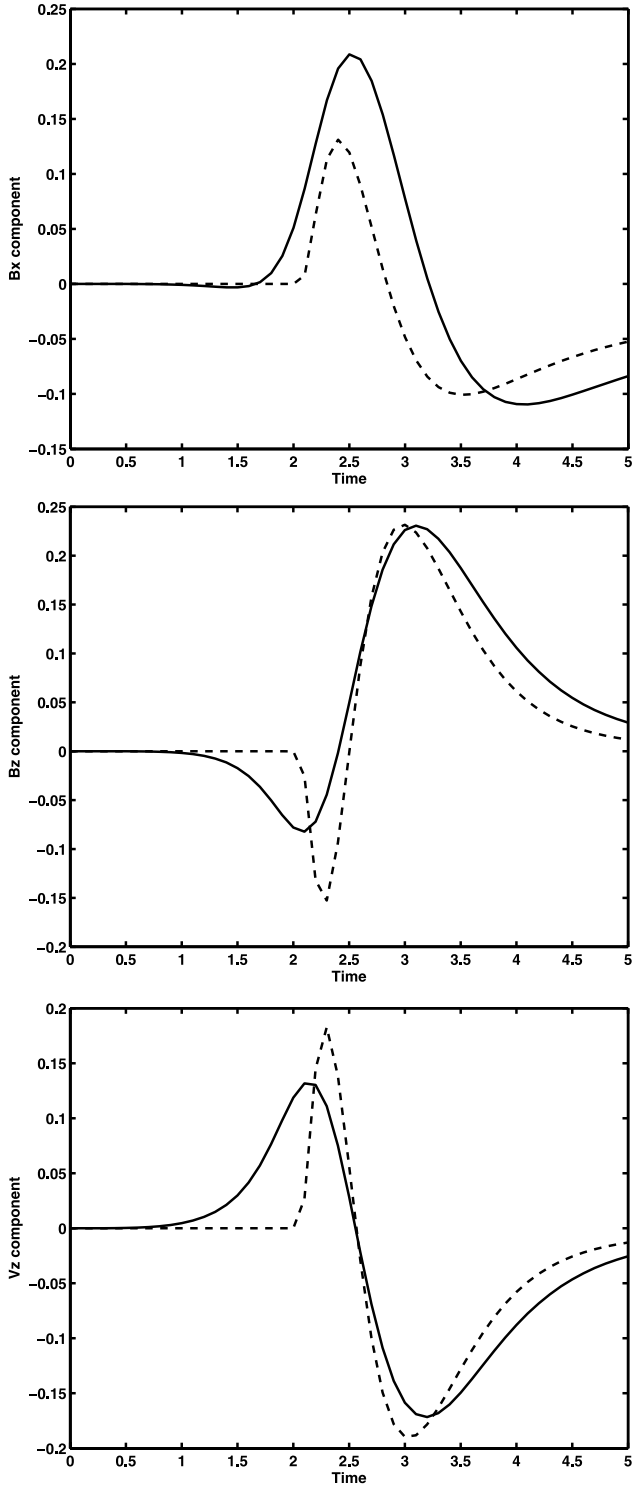

Figure 10. Comparison of the x component (upper panel) and the z component (middle panel) of the magnetic field and the z component of the plasma velocity (lower panel) for $z = 0.5$ for incompressible plasma (solid line) and compressible plasma with $\beta = 0.1$ (dashed line).

case, the incompressible model reproduces the B_z component satisfactory. Additionally, we see that the duration of the features in compressible plasma is getting shorter. This is favorable because in Figures 7 and 8 it can be seen that the incompressible model gives broader curves compared to the measurements.

[35] For the B_x component, the situation is somewhat different. From the middle panel of Figure 10 it is evident that the amplitude of the variations of the B_x component are overestimated in the incompressible theory by a factor of 2, which we also found by comparing the model results with the measured data. This is because the variations of B_x depend mainly on the size of the shocks bounding the outflow region, which will be smaller if the plasma is assumed to be compressible. Therefore the incompressible model overestimates the variations in the B_x component. For the z component of the plasma flow, the upper panel of Figure 10 shows that in compressible plasma, the amplitude is slightly increasing, while the duration is getting slightly shorter.

[36] Future work on this topic will mainly deal with the extension of the model to compressible plasma. Direct models for compressible plasma exist [*Heyn and Semenov*, 1996; *Semenov et al.*, 2004a], but it is necessary to rewrite the solution in form of a convolution integral over time in order to solve the inverse problem. Additionally, a comparison of the results with a numerical magnetotail model should clarify the influence of an inhomogeneous distribution of the plasma density and the finite thickness of the plasma sheet.

[37] In the presented work, a method to reconstruct the reconnection rate from satellite measurements outside of the plasma sheet is shown. We found that the variations observed by the Cluster spacecrafts outside of the plasma sheet boundary are consistent with the impulsive model of magnetic reconnection used in this work. The characteristic bipolar variation of the B_z component and the anticorrelated behavior of the perpendicular plasma flow velocity is reproduced. Application to three NFTE events on 8 September 2002, measured by the Cluster satellites gives an amplitude of the reconnection electric field in the range of 1–2 mV/m. The time duration of the reconnection pulse is in the order of 20–30 s, while the reconnection site is located at about 29–31 R_E tailward.

Appendix A: Derivation of the Displacement Vector

A1. Displacement Vector in Laplace-Fourier Space

[38] We can introduce a displacement vector ξ, which gives the first-order velocity and magnetic field as [*Heyn and Semenov*, 1996]

$$\mathbf{v} = \frac{\partial}{\partial t}\,\boldsymbol{\xi}\,,$$

and

$$\mathbf{B} = \left(\mathbf{B}^{(\mathbf{0})}\cdot\nabla\right)\boldsymbol{\xi}\,.$$

If we apply a Laplace-Fourier transformation to the linearized equation of motion (3) and substitute the expressions for the displacement vector (7) and (8), it is found that the z component of the displacement vector fulfills the Laplace equation. In Fourier-Laplace ($\mathcal{F}$-$\mathcal{L}$) space this can be written as an ordinary differential equation [*Heyn and Semenov*, 1996]

$$\frac{\partial^2 \xi_z}{\partial z^2} - k^2 \xi_z = 0\,. \tag{A1}$$

The solution of this equation in the upper half space ($z > 0$) is given as

$$\xi_z(k,p,z) = \xi_{z0}\, e^{-|k|z} \quad \forall \quad z > 0. \tag{A2}$$

To evaluate the displacement vector in the whole $\mathcal{F}$-$\mathcal{L}$ space, it is necessary to determine ξ_{z0}, which is the boundary condition for the displacement vector at $z = 0$.

[39] As was shown by several authors [e.g., *Semenov et al.*, 2004b], the solution for the reconnection problem in an incompressible plasma in the outflow region at $x > 0$ is given as

$$v_x = v_A\,; \quad v_z = 0, \tag{A3}$$

$$B_x = 0\,; \quad B_z = E(t-x), \tag{A4}$$

$$f = x \cdot E(t-x)\,, \tag{A5}$$

$$\mathbf{n} = \left(-\frac{\partial}{\partial x} f, 1\right), \tag{A6}$$

where (A3) is the plasma velocity, (A4) is the magnetic field inside the outflow region, (A5) determines the shape of the Petschek-type shock in the first quadrant, and $E(t)$ is the reconnection electric field along the reconnection line, while (A6) gives the unit normal to the shock. The solution for $x < 0$ can be found from symmetry considerations.

[40] If we match the magnetic field in the inflow region $\mathbf{B} = (1 + B_x, B_z)$ and the outflow region (A4) by using the Rankine-Hugoniot condition that B_n does not change across the shock, the first-order z component of the magnetic field is found as

$$B_z = 2\,\mathrm{sgn}\,(x)\,E(t-|x|) - x\,E'(t-|x|)\,, \tag{A7}$$

where the prime indicates a differentiation with respect to the argument. This equation represents the boundary condition for the magnetic field in the inflow region and can be matched with the definition of the displacement vector (8) to get the z component of the displacement vector for $z = 0$ as

$$B_z = B^{(0)}\,\frac{\partial}{\partial x}\,\xi_{z0}\,. \tag{A8}$$

After integration, the coordinate-time representation of the displacement vector at $z = 0$ is given as

$$\xi_{z0}(x,t) = \frac{1}{B^{(0)}}\left[-F(t-|x|) + |x|E(t-|x|)\right], \tag{A9}$$

where

$$F(t) = \int_0^t E(\tau)\,d\tau\,, \tag{A10}$$

is the reconnected flux.

[41] Since equation (A2) is given in $\mathcal{F}$-$\mathcal{L}$ space, it is necessary to apply a $\mathcal{F}$-$\mathcal{L}$ transformation to equation (A9). Thus the z component of the displacement vector in $\mathcal{F}$-$\mathcal{L}$ space (A2) can be written as

$$\xi_z(k,p,z) = -\frac{4\,p\,k^2}{B^{(0)}\left(p^2+k^2\right)^2}\,F(p)\,e^{-|k|z}\,. \tag{A11}$$

A2. Displacement Vector in Coordinate-Time Representation

[42] To calculate physical quantities like the magnetic field or the plasma velocity, the displacement vector must be written in coordinate-time representation. This can be done by using the Cagniard-deHoop method, which allows to perform the inverse Fourier transformation analytically, and gives the solution in form of a convolution integral in time. If we apply an inverse Fourier transformation to equation (A11) and perform a variable transformation $k = s\,p$ [*Heyn and Semenov*, 1996], we achieve

$$\xi_z(x,p,z) = -\frac{4}{2\,\pi\,B^{(0)}}\int_{-\infty}^{\infty}\frac{s^2}{\left(1+s^2\right)^2}F(p)\,e^{-spz+ispx}ds\,. \tag{A12}$$

Since $\xi(-x,\ p,\ z) = \xi^*(x,\ p,\ z)$, the integration can be rewritten as

$$\xi_z(x,p,z) = -\frac{4}{\pi\,B^{(0)}}\Re\int_0^{\infty}\frac{s^2}{\left(1+s^2\right)^2}F(p)\,e^{-p\,\tau(s)}\,ds\,, \tag{A13}$$

where we substituted

$$\tau(s) = s\,z - i\,s\,x\,. \tag{A14}$$

We can use the Cauchy theorem to deform the contour in the complex s plane in a way that $\tau(s)$ becomes real along the whole integration path. In this case, it is obvious that we can apply the shift theorem for a Laplace transformation,

$$\mathcal{L}(\Phi(t-a)) = e^{-p\,a}\Phi(p) \quad \text{for} \quad a \in \mathbb{R}.$$

Using this, equation (A13) is found to be

$$\xi_z(x,z,t) = -\frac{4}{\pi\,B^{(0)}}\Re\int_{\mathcal{C}}\frac{s^2}{\left(1+s^2\right)^2}F(t-\tau(s))\,ds\,, \tag{A15}$$

Owing to the condition of causality of the electric field and the reconnected flux ($F(t-\tau(s)) \equiv 0$ if $t-\tau(s) \le 0$), we can define an upper limit $s_{\max}$ for the integration along $\mathcal{C}$ when $t = \tau(s)$. After a variable transformation $s \to \tau$, the displacement vector in coordinate-time representation is given as the convolution integral

$$\xi_z(x,z,t) = -\frac{4}{\pi\,B^{(0)}}\Re\int_0^{t}\frac{\tau^2\,q}{\left(q^2+\tau^2\right)^2}F(t-\tau)\,d\tau\,, \tag{A16}$$

where $q = z - i\,x$.

[43] **Acknowledgments.** The authors thank A. Runov for fruitful discussions. This work is supported by the RFBR grants 04-05-64935 and 03-05-20012 BNTS, by the Austrian "Fonds zur Förderung der wissenschaftlichen Forschung" under project P17099-N08, and by project I.12/04 from the "Österreichischer Austauschdienst." V.S.S. acknowledges financial support from the Technical University Graz and the hospitality of the Institut für Theoretische Physik during scientific visits to Graz. T.P. acknowledges support by the "Österreichische Forschungsgemeinschaft" and by a Paul-Urban scholarship from the Institute of Physics of the University of Graz during visits in St. Petersburg. V.V.I. acknowledges support by INTAS "Fellowship Grant for Young Scientists" 04-83-3816 and by the Nansen community. Part of the work by R.N. and V.A.S. is supported by INTAS 03-51-2728 grant. Also acknowledged is support by the Austrian Academy of Sciences, "Verwaltungsstelle für Auslandsbeziehungen."

[44] Lou-Chuang Lee thanks Tsugunobu Nagai and Jean-Andre Sauvaud for their assistance in evaluating this paper.

References

Balogh, A., et al. (2001), The Cluster magnetic field investigation: Overview of in-flight performance and initial results, *Ann. Geophys.*, *19*, 1207–1217.

Biernat, H. K., M. F. Heyn, and V. S. Semenov (1987), Unsteady Petschek reconnection, *J. Geophys. Res.*, *92*, 3392–3396.

Blanchard, G. T., L. R. Lyons, O. de la Beaujardière, R. A. Doe, and M. Mendillo (1996), Measurments of the magnetotail reconnection rate, *J. Geophys. Res.*, *101*, 15,265–15,276.

Blanchard, G. T., L. R. Lyons, and O. de la Beaujardière (1997), Magnetotail reconnection rate during magnetospheric substorms, *J. Geophys. Res.*, *102*, 24,303–24,312.

Cagniard, L. (1939), *Reflexion et Refraction des Ondes Seismiques Progressive* (in French), Gauthier–Villard, Paris. (English translation by E. A. Flinn and C. H. Dix, *Reflection and Refraction of Progressive Seismic Waves*, McGraw-Hill, New York, 1962.)

deHoop, A. T. (1960), The surface line source problem, *Appl. Sci. Res., Ser. B*, *8*, 349–356.

Farrugia, C. J., R. C. Elphic, D. J. Southwood, and S. W. H. Cowley (1987), Field and flow perturbations outside the reconnected field line region in flux transfer events: Theory, *Planet. Space Sci.*, *35*, 227–240.

Hadamard, J. (1932), *Le Problème de Cauchy et les Équations aux Dérivées Partielles Lineaires Hyperboliques*, Hermann, Paris.

Haerendel, G., G. Paschmann, N. Sckopke, H. Rosenbauer, and P. C. Hedgecock (1978), The frontside boundary layer of the magnetopause and the problem of reconnection, *J. Geophys. Res*, *83*, 3195–3216.

Harvey, C. C. (1998), Spatial gradients and the volumetric tensor, in *Analysis Methods for Multi-Spacecraft Data*, edited by G. Paschmann and P. W. Daly, *Rep. SR–001*, Int. Space Sci. Inst., Bern, Switzerland.

Hau, L. N., and B. U. Ö. Sonnerup (1999), Two-dimensional coherent structures in the magnetopause: Recovery of static equilibria from single-spacecraft data, *J. Geophys. Res.*, *104*, 6899–6918.

Heyn, M. F., and V. S. Semenov (1996), Rapid reconnection in compressible plasma, *Phys. Plasmas*, *3*, 2725–2741.

Heyn, M. F., H. K. Biernat, R. P. Rijnbeek, and V. S. Semenov (1988), The structure of reconnection layers, *J. Plasma Phys.*, *40*, 235–252.

Hu, Q., and B. U. Ö. Sonnerup (2001), Reconstruction of magnetic flux ropes in the solar wind, *Geophys. Res. Lett.*, *28*, 467–470.

Hu, Q., and B. U. Ö. Sonnerup (2003), Reconstruction of two-dimensional structures in the magnetopause: Method improvements, *J. Geophys. Res.*, *108*(A1), 1011, doi:10.1029/2002JA009323.

Ieda, A., S. Machida, T. Mukai, Y. Saito, T. Yamamoto, A. Nishida, T. Terasawa, and S. Kokubun (1998), Statistical analysis of plasmoid evolution with GEOTAIL observations, *J. Geophys. Res.*, *103*, 4453–4465.

Lamb, H. (1904), On the propagation of tremors over the surface of an elastic solid, *Phil. Trans. R. Soc. London, Ser. A*, *203*, 1–42.

Lawrence, G. R., R. P. Rijnbeek, and V. S. Semenov (2000), Remote sensing of flux transfer events: Investigations of theoretical constraints based on model magnetopause time series data, *J. Geophys. Res.*, *105*, 7629–7638.

Nagai, T., I. Shinohara, M. Fujimoto, M. Hoshino, Y. Saito, S. Machida, and T. Mukai (2001), Geotail observations of the Hall current system: Evidence for magnetic reconnection in the magnetotail, *J. Geophys. Res.*, *106*, 25,929–25,950.

Østgaard, N., J. Moen, S. B. Mende, H. U. Frey, T. J. Immel, P. Gallop, K. Oksavik, and M. Fujimoto (2005), Estimates of magnetotail reconnection rate based on IMAGE FUV and EISCAT measurements, *Ann. Geophys.*, *23*, 123–134.

Petschek, H. E. (1964), Magnetic field annihilation, in *Physics of Solar Flares*, edited by W. N. Hess, *NASA Spec. Publ.*, *50*, 425–440.

Rème, H., et al. (2001), First multispacecraft ion measurements in and near the Earth's magnetosphere with the identical Cluster ion spectrometry (CIS) experiment, *Ann. Geophys.*, *19*, 1303–1354.

Runov, A., et al. (2003), Current sheet structure near magnetic X–line observed by Cluster, *Geophys. Res. Lett.*, *30*(11), 1579, doi:10.1029/2002GL016730.

Russell, C. T., and R. C. Elphic (1978), Initial ISEE magnetometer results: Magnetopause observations, *Space Sci. Rev.*, *22*, 681–715.

Semenov, V. S., I. V. Kubyshkin, V. V. Lebedeva, R. P. Rijnbeek, M. F. Heyn, H. K. Biernat, and C. J. Farrugia (1992), A comparison and review of steady-state and time-varying reconnection, *Planet. Space Sci.*, *40*(49), 63–87.

Semenov, V. S., M. F. Heyn, and I. B. Ivanov (2004a), Magnetic reconnection with space and time varying reconnection rates in a compressible plasma, *Phys. Plasmas*, *11*, 62–70.

Semenov, V. S., I. V. Kubyshkin, R. P. Rijnbeek, and H. K. Biernat (2004b), Analytical theory of unsteady Petschek-type reconnection, in *Physics of Magnetic Reconnection in High-Temperature Plasmas*, edited by M. Ugai, pp. 35–68, Res. Signpost, Trivandrum, India.

Semenov, V. S., T. Penz, M. F. Heyn, I. B. Ivanov, I. V. Kubyshkin, H. K. Biernat, V. V. Ivanova, and R. P. Rijnbeek (2005), Reconstruction of the reconnection rate from magnetic field disturbances in an incompressible plasma, in *Solar-Planetary Relations*, edited by H. K. Biernat et al., pp. 261–302, Res. Signpost, Trivandrum, India.

Sergeev, V. A., V. S. Semenov, and M. V. Sidneva (1987), Impulsive reconnection in the magnetotail during substorm expansion, *Planet. Space Sci.*, *35*, 1199–1212.

Sergeev, V. A., R. C. Elphic, F. S. Mozer, A. Saint-Marc, and J. A. Sauvaud (1992), A two-satellite study of nightside flux transfer events in the plasma sheet, *Planet. Space Sci.*, *40*, 1551–1572.

Sergeev, V. A., et al. (2005), Transition from substorm growth to substorm expansion phase as observed with a radial configuration of ISTP and Cluster spacecraft, *Ann. Geophys.*, *23*, 2183–2198.

Slavin, J. A., R. P. Lepping, J. Gjerloev, D. H. Fairfield, M. Hesse, C. J. Owen, M. B. Moldwin, T. Nagai, A. Ieda, and T. Mukai (2003), Geotail observations of magnetic flux ropes in the plasma sheet, *J. Geophys. Res.*, *108*(A1), 1015, doi:10.1029/2002JA009557.

Sonnerup, B. U. Ö., H. Hasegawa, and G. Paschmann (2004), Anatomy of a flux transfer event seen by Cluster, *Geophys. Res. Lett.*, *31*, L11803, doi:10.1029/2004GL020134.

Southwood, D. J. (1985), Theoretical aspects of ionosphere-magnetosphere-solar wind coupling, *Adv. Space Res.*, *5*, 7–14.

Tikhonov, A. N., and V. Y. Arsenin (1977), *Solutions of Ill-Posed Problems*, John Wiley, Hoboken, N. J.

Walthour, D. W., B. U. Ö. Sonnerup, G. Paschmann, H. Lühr, D. Klumpar, and T. Potemra (1993), Remote sensing of two-dimensional magnetopause structures, *J. Geophys. Res.*, *98*, 1489–1504.

Walthour, D. W., B. U. Ö. Sonnerup, R. C. Elphic, and C. T. Russell (1994), Double vision: Remote sensing of a flux transfer event with ISEE 1 and 2, *J. Geophys. Res.*, *99*, 8555–8563.

H. K. Biernat, R. Nakamura, and T. Penz, Space Research Institute, Austrian Academy of Sciences, A-8042 Graz, Austria. (thomas.penz@oeaw.ac.at)

M. F. Heyn, Institute for Theoretical Physics, Technical University Graz, A-8010 Graz, Austria.

I. B. Ivanov, Petersburg Nuclear Physics Institute, Gatchina, 188300 Russia.

V. V. Ivanova, I. V. Kubyshkin, V. S. Semenov, and V. A. Sergeev, Institute of Physics, State University St. Petersburg, St. Petersburg, 198504 Russia.